Investigation of PEM fuel cell performance using the bio-inspired flow field combined with baffles on branch channels

Cite as: AIP Conference Proceedings **2187**, 020004 (2019); https://doi.org/10.1063/1.5138259
Published Online: 10 December 2019

A'rasy Fahruddin, Djatmiko Ichsani, Fadlilatul Taufany, and Budi Utomo Kukuh Widodo

Investigation of PEM Fuel Cell Performance Using the Bio-Inspired Flow Field Combined with Baffles on Branch Channels

A'rasy Fahruddin[1, a)], Djatmiko Ichsani[1, b)], Fadlilatul Taufany[2], and Budi Utomo Kukuh Widodo[1]

[1] Mechanical Engineering Department, Institut Teknologi Sepuluh Nopember (ITS), 60111, Surabaya, Indonesia
[2] Chemical Engineering Department, Institut Teknologi Sepuluh Nopember (ITS), 60111, Surabaya, Indonesia
.
[a)]*Corresponding author: arasy.fahruddin@umsida.ac.id*
[b)]*djatmiko@me.its.ac.id*

Abstract. Fuel cell is one of the energy conversion devices that can be an alternative to dealing with fossil energy depletion and environmental issues. The aim of this study is to determine the effect of baffles on branch channels on leaf shape flow fields towards PEM fuel cell performance. Numerical studies were applied to 3d models with 25 cm² active area. The distance between baffles in the branch channel is varied with the height of the baffles as a reference. The results show that the shorter the distance between baffles, the higher the current density and pressure drop produced. However, a decrease in pressure drop occurs at a distance of 20h.

INTRODUCTION

The issue of limited petroleum reserves and air pollution concerns encourage researchers to innovate new design of energy conversion machines with alternative energy sources and environmentally friendly. Fuel cell is alternative technologies that can be chosen because fuel cells use hydrogen as an energy source to be converted into electrical energy directly. Hydrogen is a renewable energy because it can be produced by an electrolysis system. Polymer Electrolyte Membrane (PEM) fuel cell is a simple fuel cell that can work optimally at relatively low temperatures [1], so PEM fuel cells are easily applied to portable electronic devices and transportation devices.

PEM fuel cell devices have prices that are still relatively expensive, one way to reduce prices is to increase cell performance with the same dimensions. The design of flow fields is an important factor that influences cell performance. The bio-inspired flow field design has been investigated by Roshandel (2012), and the results show a power density increase up to 56% compared to conventional flow field parallel [2]. In other cases, Ozden (2017) has tried using flow field inspired leaf shapes in DMFC (Direct Methanol Fuel Cell). The serpentine flow field arrangement on the anode side and leaf shape on the cathode side shows the best performance [3].

The use of baffles in the channel in the flow field is also proven to be able to improve performance of the PEM fuel cell [4–7]. Heidary (2016) has investigated the effect of baffles in parallel flow fields and cell performance can increase up to 11% [4]. However, the use of baffles on bio-inspired flow fields has not been studied. Therefore, in this

Innovative Science and Technology in Mechanical Engineering for Industry 4.0
AIP Conf. Proc. 2187, 020004-1–020004-7; https://doi.org/10.1063/1.5138259
Published by AIP Publishing. 978-0-7354-1934-6/$30.00

study we investigated the effect of using baffles on branch channels in flow field inspired by leaf towards cell performance.

METHOD

The area of active PEM fuel cell used is 25 cm². The design of the serpentine flow field is used on the anode side, while on the cathode side the leaf shape design is used. In the cathode flow field, the use of baffles on the branch channel is investigated with the configuration according to **FIGURE 1**. Spacing between baffles is set based on the height of the baffle (h = 0.5 mm) which is 10h, 20h and 30h. Baffle is also installed on the mother channel to block the flow directly to the output. The operating condition is set at a temperature of 60˚C and a pressure of 1 atm. The hydrogen input flow mass is 6.10^{-7} Kg/s while the input air is 2.10^{-5} Kg/s.

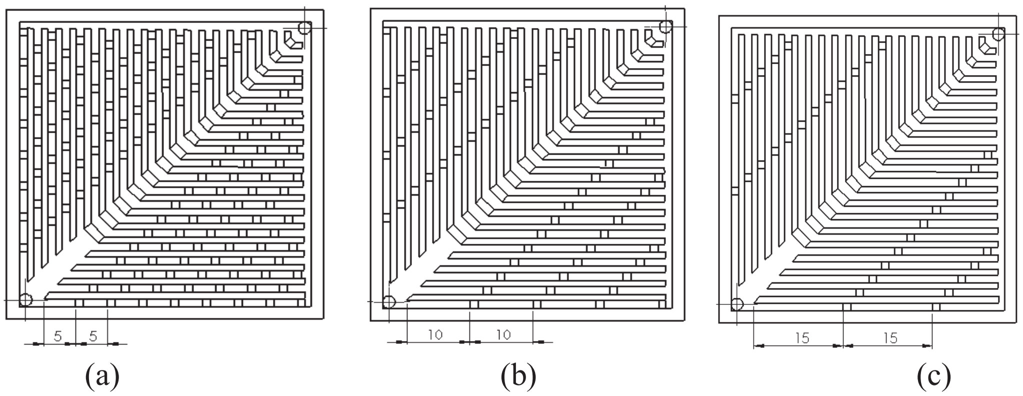

FIGURE 1. Baffle configuration on branch channels. (a) Space 10h, (b) Space 20h, (c) Space 30h.

This study applies numerical simulation using Ansys-Fluent with the add-on module Fuel Cell PEM (Polymer Electrolyte Membrane) type. Discrete solvers are used to increase the convergence of simulations. This simulation is using SIMPLE (Semi-Implicit Method with Pressure Linked Equations) method, least squares cell based gradient, standard discretization for pressure and first-order upwind for other parameters. The F-cycle is choosing for multi-grid cycle with BCGSTAB (Bi-Conjugate Gradient Stabilized) as a stabilization method for potential equations and species. Additionally, the tolerance of multi-grid cycles is reduced to 0.001 for several numerical equations, as suggested in the Ansys module manual [8].

The open circuit voltage on PEMFC is used 1.05 V in CFD simulations. The electrical potential for the cathode is varied starting from 0.8 V. Then, the electrical potential is reduced to 0.2 V gradually, by a difference of 0.2 V. This way we will obtain variable current density data, so that a polarization curve can be drawn. The full model parameters are written in **TABLE 1**.

Governing equation

Following is the transport equation used as governing equation [4]:

$$\nabla.\left(\rho\varphi\vec{V}\right) = \nabla.\left(\Gamma_\varphi \nabla\varphi\right) + S_\varphi \tag{1}$$

where ρ is density of the mixture, $\vec{V}$ is velocity, φ is quantity of transport (mass, momentum, energy), Γ_φ is diffusivity, and S_φ is the source term. From the Butler-Volmer equation, electrical current at anode and cathode side, *Ra* and *Rc,* can be obtained [4]:

$$R_a = \zeta_a\, j_a^{ref} \left(\frac{[H_2]}{[H_2]_{ref}}\right)^{\gamma_a} \left(e^{\frac{\alpha_a F \eta_a}{RT}} - e^{-\frac{\alpha_c F \eta_a}{RT}}\right) \tag{2}$$

$$R_c = \zeta_c\, j_c^{ref} \left(\frac{[O_2]}{[O_2]_{ref}}\right)^{\gamma_c} \left(-e^{\frac{\alpha_a F \eta_c}{RT}} + e^{-\frac{\alpha_c F \eta_c}{RT}}\right) \tag{3}$$

where ζ is a specific active surface area, j_{ref} is reference exchange current density per active surface area, α_a and α_c are transfers coefficients at the anodes and cathode, γ_a and γ_c are concentration exponents at anode and cathode, η_a and η_c are overpotentials at the anode and cathode, and V_{oc} is open circuit voltage.

TABLE 1. Simulation model parameters [9].

Property	Value	Unit
Membrane thermal conductivity	0.16	W/mK
Dry membrane density	1980	Kg/m^3
Catalyst layer porosity	0.4	
Catalyst surface to volume ratio	$1.127 x 10^7$	$m^2.Pt/m^3$
Gas diffusion layer density	321.5	Kg/m^3
Gas diffusion layer electric conductivity	280	1/ohm.m
Gas diffusion layer porosity	0.6	
Open circuit voltage	1.05	V
Anode Reference concentration	0.0008814	$kmol/m^3$
Cathode Reference concentration	0.0008814	$kmol/m^3$
Anode charge transfer coefficient	1	
Cathode charge transfer coefficient	1	
Anode reference current density	7.17	A/m^2. Pt
Cathode reference current density	$7.17 x 10^5$	A/m^2. Pt

RESULT AND DISCUSSION

From **FIGURE 2** we can see that installing baffles on the channel can increase current density significantly compared to without baffle, up to 15%. Baffle spacing on branch channels does not affect cell performance at the macro scale. But on a more precise scale the difference in performance can be seen. The closer the space between the baffles the greater the current density that is generated both at medium voltage (0.4 V) and at low voltage (0.2 V). This is because the closer the space between the baffles, the more baffles, so that more air is forced towards the membrane [4–6]. More amount of air supply in the membrane will increase the electric current that can be produced.

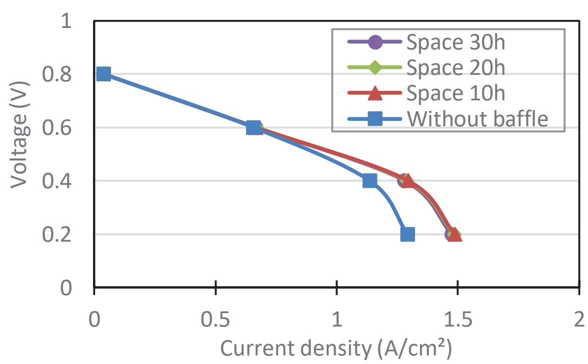

FIGURE 2. Polarization diagram

FIGURE 3 shows the distribution of oxygen mass fractions in the three flow field designs with different baffle distances on the branch channel. The difference in the distance between baffles on the branch channel apparently did not have a significant effect on the distribution of oxygen mass fractions on a macro scale. This can be caused by the flow in the branch channel has a relatively low flow rate so that collisions with baffles are relatively small [5].

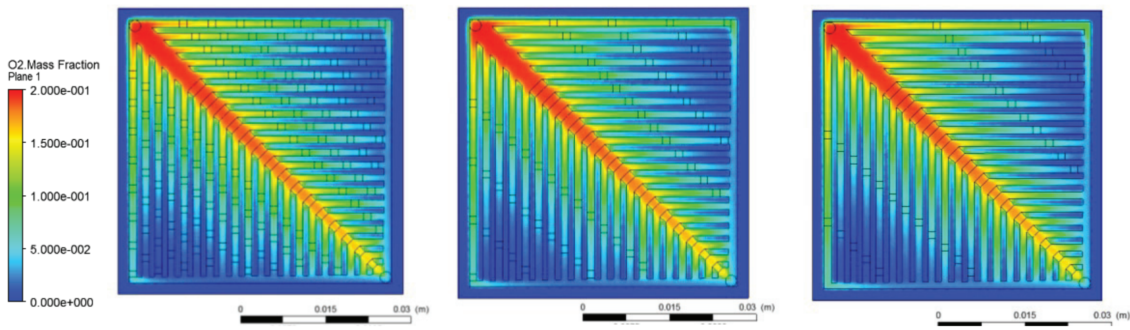

(a) (b) (c)

FIGURE 3. Oxygen mass fraction distribution with variations in distance between baffles, (a) Distance between baffles 5 mm, (b) Distance between baffles 10 m, (c) Distance between baffles 15 mm.

Data samples at several positions were taken to show the value of oxygen mass fraction, because the distribution in **FIGURE 3** did not show any difference. The position of the data sample taken is on several lines along the z axis and along the x axis as shown in **FIGURE 4** below.

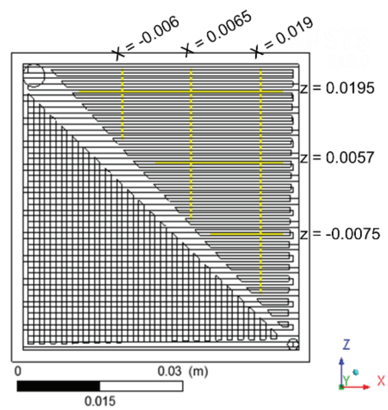

FIGURE 4. Position of the sample data on the distribution of oxygen mass fractions.

FIGURE 5 shows the value of the mass fraction at the position along the z axis, at x = -0.006 (a), at x = 0.0065 (b), at x = 0.019 (c), and along the x-axis, at z = -0.0075 (d), at z = 0.0057 (e), at z = 0.0195 (f). From these graphs it can be seen that the 10h baffle distance tends to produce the highest mass fraction value, the 20h baffle distance in the second, and the 30h baffle distance tend to be the lowest. The shorter the distance between the baffles the greater the oxygen flow in the direction of the gas diffusion layer, so that the mass fraction of oxygen in the gas diffusion layer is greater.

The effect of the distance between baffles on cell performance can be seen with a more thorough scale. **FIGURE 6** shows the effect of the distance between baffles to the current density at a working voltage of 0.4 V. The farther distance between baffles shows the lower cell performance. However, the difference in performance between 10h and 20h is lower than the difference in performance between 20h and 30h, from this phenomenon it can be predicted that there will be a maximum point where the smaller the distance between baffles will no longer increase cell performance.

The closer the distance between baffles, the more number of baffles in one branch channel. The closer the distance between the baffles and the more baffles, the reactant pressure to the catalyst layer will be greater, so that the oxygen supply will be more thereby cell performance can be increased.

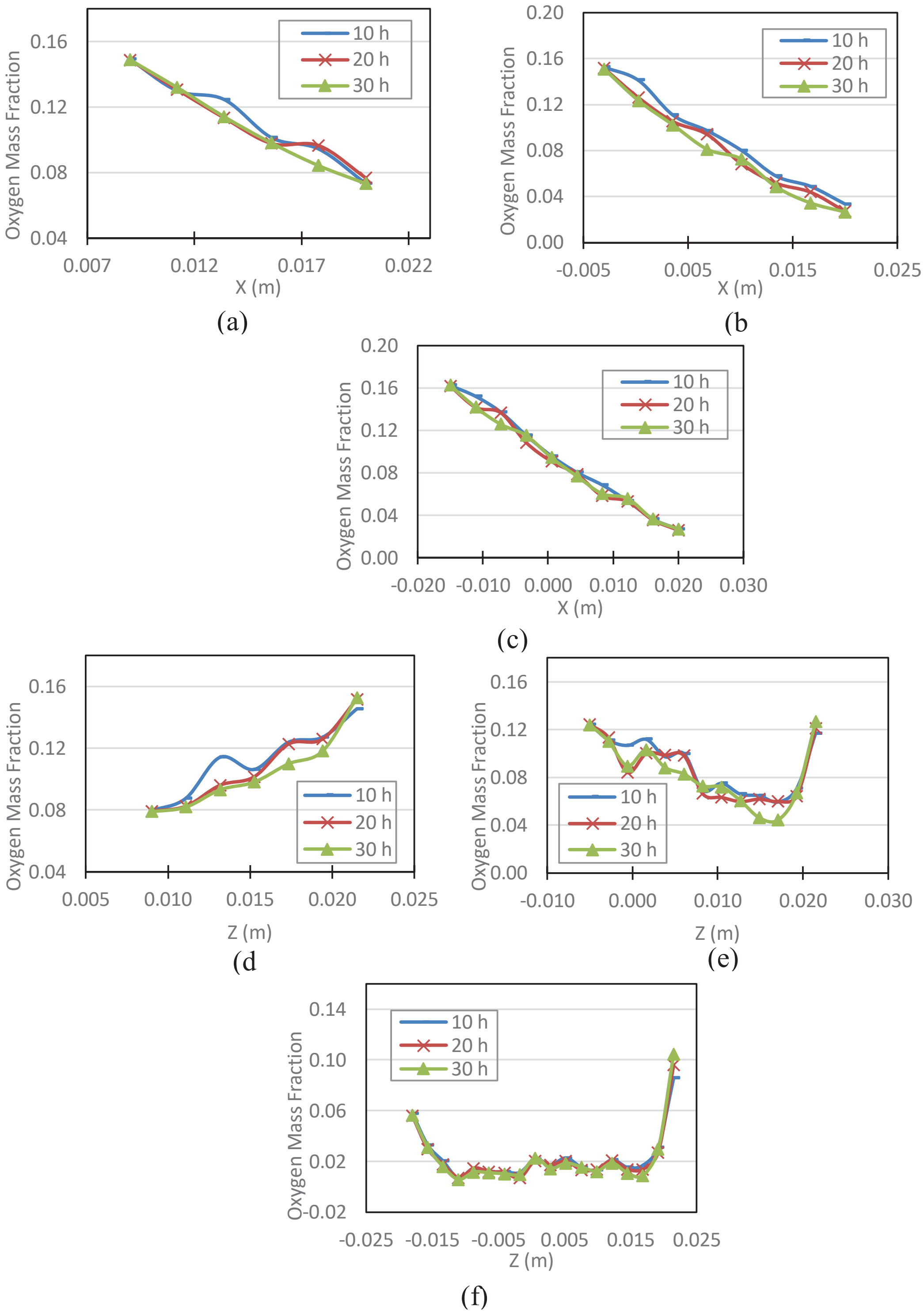

FIGURE 5. Oxygen mass fraction at sample points. Along the z axis: (a) at x = -0.006, (b) at x = 0.0065, (c) at x = 0.019. Along the x-axis: (d) at z = -0.0075, (e) at z = 0.0057, (f) at z = 0.0195.

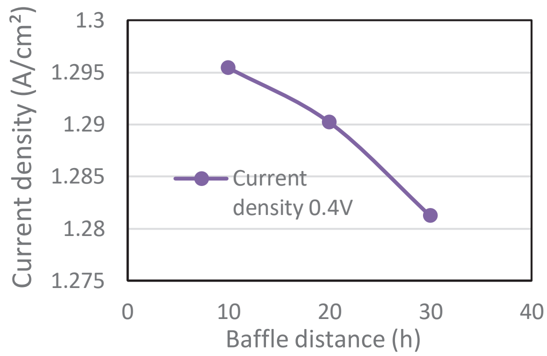

FIGURE 6. Effect of baffle distance on current density at 0.4 V.

The large uniformity of oxygen mass fraction and uniformity of flow velocity are the causes of high current density. The smaller the distance between baffles will reduce the uniformity of the fluid pressure. **TABLE 2** shows the uniformity index for each baffle distance variation.

TABLE 2. Uniformity index for some parameters on the cathode side.

Index Uniformity	10 h	20 h	30 h
Oxygen Mass Fraction	0.589	0.583	0.578
Static Pressure	0.830	0.830	0.839
Velocity Magnitude	0.519	0.510	0.506
Temperature	0.997	0.997	0.997

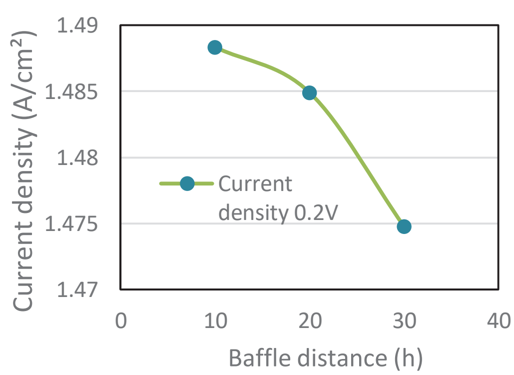

FIGURE 7. Effect of baffle distance on current density at 0.2 V voltage.

FIGURE 7 shows the effect of the distance between baffles to the current density at a working voltage of 0.2 V. The greater the distance between baffles the smaller the current density can be achieved. As in the previous discussion, this is because of the wider the distance between the baffles, the less pressure to the catalyst layer. So that the oxygen supply is smaller and the resulting current density will be lower.

FIGURE 8 shows the amount of pressure drop in the variation of the baffle distance. Small baffle spacing results in the greatest pressure drop, because the more baffle the channel gets narrower. The 20h baffle distance produces a lower pressure drop than the 30h baffle distance, this might happen because higher speeds make it easier to push air vapor [10]. In addition, a wider space formed between baffles at a 30h baffle distance has the potential to cause greater pressure due to fluid buildup in the rear baffles and cause back pressure. This needs to be further investigated.

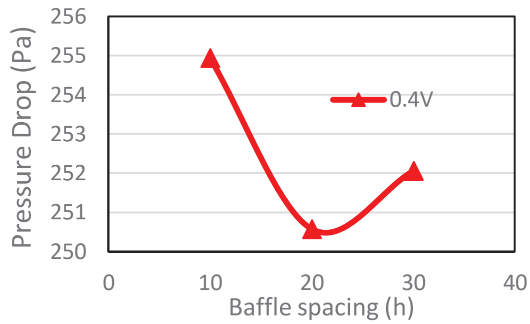

FIGURE 8. Pressure drop on the cathode side.

The amount of fluid density in each variation of baffle distance can be seen in **TABLE 3**. The 10h baffle distance produces the largest current density so that it will produce the greatest heat, the water vapor produced will also be more so that the fluid density will be the highest. A smaller baffle distance will produce a narrower channel resulting in a higher average speed.

TABLE 3. Average value of several parameters in the fluid on the cathode side.

Average in cathode side	10 h	20 h	30 h	
Fluid velocity	1.476	1.405	1.385	m/s
Fluid temperature	333.605	333.597	333.588	K
Fluid density	0.9046	0.9042	0.9038	Kg/m³

CONCLUSION

The installing baffles on the channel can increase current density significantly compared to without baffle, up to 15%. The closer the space between the baffles the greater the current density that is generated both at medium voltage (0.4 V) and at low voltage (0.2 V). This is because the closer the space between the baffles, the more baffles, so that more air is forced towards the membrane. The shorter the distance between baffles, the higher the pressure drop produced. However, the decline occurred at a distance of 20h. This might happen because higher speeds make it easier to push air vapor.

ACKNOWLEDGEMENT

The authors acknowledge Lembaga Penelitian dan Pengabdian Masyarakat Institut Teknologi Sepuluh Nopember (LPPM-ITS) Indonesia for funding this research.

REFERENCES

1. Arvay, A., French, J., Wang, J., Peng, X., Kannan, A.M., Int. J. Hydrogen Energy, 38, (9), pp. 3717–3726 (2013).
2. Roshandel, R., Arbabi, F., Moghaddam, G.K., Renew. Energy, 41, pp. 86–95 (2012).
3. Ozden, A., Ercelik, M., Ouellette, D., Colpan, C.O., Int. J. Hydrogen Energy, 42, (33), pp. 21546–21558 (2017).
4. Heidary, H., Kermani, M.J., Prasad, A.K., Advani, S.G., Dabir, B., Int. J. Hydrogen Energy, 42, (4), pp. 2265–2277 (2016).
5. Ghanbarian, A., Kermani, M.J. Energy Convers. Manag., 110, pp. 356–366 (2016).
6. Heidary, H., Kermani, M.J., Dabir, B. Energy Convers. Manag., 124, pp. 51–60 (2016).
7. Fahruddin, A., Ichsani, D., Taufany, F. MATEC Web Conf., 197, p. 8010 (2018).
8. Ansys.Inc: 'ANSYS Fluent Fuel Cell Modules Manual' (Ansys.Inc, 2013)
9. Limjeerajarus, N., Charoen-amornkitt, P. Int. J. Hydrogen Energy, 40, (22), pp. 7144–7158 (2015).
10. Xing, L., Cai, Q., Xu, C., Liu, C., Scott, K., Yan, Y. Energy, 106, pp. 631–645 (2016).